ceramics

MDPI

Article

On the Enlargement of the Emission Spectra from the $^4I_{13/2}$ Level of Er^{3+} in Silica-Based Optical Fibers through Lanthanum or Magnesium Co-Doping

Manuel Vermillac, Jean-François Lupi, Stanislaw Trzesien, Michele Ude and Wilfried Blanc *

Université Côte d'Azur, INPHYNI, CNRS UMR7010, Parc Valrose, 06108 Nice, France; manuel.vermillac@ec-nantes.fr (M.V.); lupijeanfrancois@gmail.com (J.-F.L.); stanislaw.trzesien@unice.fr (S.T.); Michele.ude@unice.fr (M.U.)

* Correspondence: wilfried.blanc@unice.fr

Received: 14 November 2018; Accepted: 6 December 2018; Published: 11 December 2018

Abstract: Improving optical fiber amplifiers requires the elaboration and use of new materials and new compositions. In this sense, we prepared erbium-doped optical fiber samples that were co-doped with magnesium or lanthanum by gradual-time solution doping. Doping concentrations and thermal processes induce the formation of nanoparticles. The effect of lanthanum and magnesium contents on the width of the spontaneous emission of the $^4I_{13/2}$ level of Er^{3+} was characterized in the nanoparticle-rich fiber samples. For that purpose, the width was characterized by the effective linewidth and the full-width at half-maximum (FWHM). The results indicate the robustness of the effective linewidth to strong variations in the intensity profiles of the $^4I_{13/2}$ spontaneous emission. Increasing the doping concentrations of both magnesium and lanthanum increases the FWHM and the effective linewidth, along with optical losses. Results show that the fabrication of nanoparticle-rich optical fibers through lanthanum or magnesium doping induces an FHWM broadening of 54% and 64%, respectively, or an effective linewidth broadening of 59% (for both elements) while maintaining a transparency that is compatible with fiber laser and amplifier applications.

Keywords: optical fibers; silica; Er^{3+}; nanoparticles; optical properties; magnesium; lanthanum

1. Introduction

The development of new rare-earth ion (RE)-based optical fiber devices, such as amplifiers and lasers, requires improvements in their spectroscopic properties [1,2]. These properties depend on the composition and the structure of the material of the optical fiber, which is commonly based on silica glass [3–5]. For that purpose, the material is commonly modified by the addition of new elements to silica to enable, to name few examples, fluorescence lifetime enhancement, reduction in the sensitivity to photodarkening and radiodarkening, etc. [6–9]. In this context, previous studies have shown that the formation of nanoparticles allows for noticeable alterations of the spectroscopic properties of rare-earth-ion-doped silica-based optical fibers such as the fluorescence lifetime or energy transfer enhancements [10–12]. In the case of Er^{3+}, the addition of magnesium has been shown to induce the formation of magnesium-rich nanoparticles that contain luminescent ions [13]. This modified environment enables an increase in the width of the emission band from the $^4I_{13/2}$ level of Er^{3+}, which is used in the telecom band [14]. For instance, such modification is of interest for the increase in the wavelength multiplexing capacity.

The present systematic study aims to characterize the broadening of the Er^{3+} $^4I_{13/2} \rightarrow {}^4I_{15/2}$ emission band of silica-based optical fibers through the formation of lanthanum- and magnesium-rich particles. Lanthanum is used because it has already been shown to enhance the spectroscopic properties

of thulium-doped optical fibers through the formation of lanthanum-rich particles [10]. Magnesium doping was also carried out. Magnesium doping has been shown to induce the formation of magnesium-rich particles and to improve the spectroscopic properties of Er^{3+}-doped fiber samples [14]. However, discussion on the effect of magnesium has been previously limited by the presence of phosphorous, motivating this investigation.

In the present study, fibers were drawn from preforms prepared according to the gradual-time solution-doped MCVD (Modified Chemical Vapor Deposition) process [15]. Material characteristics were analyzed for the fiber samples containing amorphous particles (lanthanum- or magnesium-rich), with size increasing with Mg or La doping content [16]. Optical losses of the samples and spectroscopic properties are presented. The evolution of the spectroscopic properties of the fiber samples with the composition and optical properties is discussed. Results show that both lanthanum and magnesium doping enhance the spectroscopic properties of the fiber samples with acceptable optical losses.

2. Experimental

Two MCVD optical preforms were fabricated by the gradual-time solution doping method [15]. The core porous layer of the optical preforms was deposited at around 1535 °C by oxidizing $GeCl_4$ and $SiCl_4$ gases. The $GeCl_4/SiCl_4$ ratio and temperature slightly change during the deposition stage, which can induce minor variations in GeO_2 content along the preform. However, such variation is not expected to alter the luminescence properties of Er^{3+} ions. Following the gradual-time solution doping process, detailed in [15], the porous layer of the La preform was soaked for 1 h with an ethanol-based solution containing 0.01 mol·L^{-1} of $ErCl_3$ and $LaCl_3$. A second ethanol-based solution containing 0.01 and 0.7 mol·L^{-1} of $ErCl_3$ and $LaCl_3$, respectively, was then used to soak 26 cm of the preform, with the soaked length decreasing from 26 to 10 cm in 20 min. The remaining 10 cm of the porous layer remained soaking for a supplementary hour. The process was identical for the Mg-doped preform (36 cm long), but two different ethanol-based solutions were used. The first solution contained 0.01 and 0.1 mol·L^{-1} of $ErCl_3$ and $MgCl_2$, respectively, and the second solution contained 0.01 and 2 mol·L^{-1} of $ErCl_3$ and $MgCl_2$, respectively. Considering the purity of precursors, $ErCl_3$ (Sigma-Aldrich, St. Louis, MO, USA) was incorporated using erbium(III) chloride hexahydrate, 99.995%. $LaCl_3$ (Alfa Aesar, Haverhill, MA, USA) was from lanthanum(III) chloride heptahydrate with a 99.99% purity. $MgCl_2$ (Sigma-Aldrich) was incorporated with a 99.8% purity.

The tubes were then sintered and collapsed by several heating passes, which gradually increased in temperature up to around 2200 °C. The optical preforms have a diameter of around 1 cm. Along the length of the preforms, from the short-soaking-time side of the preform to the long-soaking-time side, both preforms exhibit longitudinal whitening of their cores (cf. Figure 1). The short-soaking-time side is transparent, the gradually soaked parts gradually whiten, and long-soaking-time side is white. This white color is correlated to the presence of scatterers, such as nanoparticles, in the core of optical fibers [10]. Both optical fibers were drawn at 124 µm, with temperature and tension at typical values of around 1940 °C and 0.30 N and 0.36 N ± 0.01 N for Mg-doped and La-doped optical fibers, respectively. The material, spectroscopic, and optical properties of fiber samples are listed in Table 1.

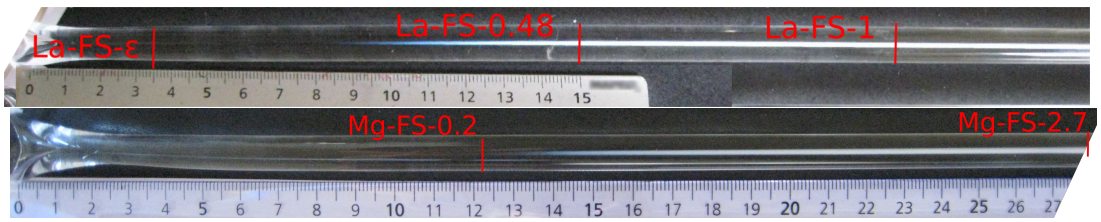

Figure 1. Pictures of the La-doped (**top**) and Mg-doped (**bottom**) optical preforms. For both preforms, the core whitens with the increase in La or Mg content along the length of the preform. Estimated positions in the preform of the extrema fiber samples are indicated by vertical lines.

Table 1. Table of characteristics of the optical fiber samples. Fiber sample names correspond to the doping element (Mg or La) and its content inside the fiber sample. Interpolated values of concentrations are marked with a "*". Ge content is also expressed.

Fiber Sample	Mg/La Content (atom %)	Ge (atom %)	Full-Width at Half-Maximum (FWHM) (nm)	$\Delta\lambda_{eff}$
La-FS-ϵ	La—undetectable	1.1	9.54	30.5
La-FS-0.17	La—0.17	0.87	26.8	42
La-FS-0.23	La—0.23	0.67	28.4	45.7
La-FS-0.31	La—0.31	0.43	29.4	46.1
La-FS-0.35	La—0.35	0.50	30.2	47
La-FS-0.46	La—0.46 *	0.5 *	31	48.5
La-FS-0.51	La—0.51 *	0.5 *	31.4	49.7
La-FS-0.58	La—0.58	0.52	31.3	49.3
La-FS-0.67	La—0.67	0.42	32.4	50.7
La-FS-1	La—1	0.26	32.3	51.8
Mg-FS-0.22	Mg—0.22	0.74	31.4	46.3
Mg-FS-0.23	Mg—0.23	0.78	30.5	46.2
Mg-FS-0.89	Mg—0.89	0.39	33.2	48.9
Mg-FS-1	Mg—1	0.39	33.3	50
Mg-FS-1.1	Mg—1.1	0.30	35.2	51.5
Mg-FS-1.3	Mg—1.3	0.34	35	52.3
Mg-FS-2.1	Mg—2.1	0.26	34.6	51.5
Mg-FS-2.3	Mg—2.3	0.26	34.7	51.9
Mg-FS-2.4	Mg—2.4	0.25	35.1	51.9
Mg-FS-2.7	Mg—2.7	0.15	34.2	50.5
Ref-Silica	La/Mg—0; P—3.7	5.8	21.4	32.8

Samples were taken along the length of the fibers every 50 m for the Mg-doped fiber and 40 m for the La-doped fiber. The difference in the spatial frequency of the sampling arises from the difference in the lengths of the Mg-doped and La-doped optical fibers produced (890 and 1080 m) and the objective to provide a homogeneous number of samples. La and Mg contents were analyzed by energy dispersive X-ray (EDX). The highest values of measured content of La and Mg in the fiber samples (measured at the center of the core) are indicated in Figure 2 and Table 1. The fiber samples were carbon coated and analyzed by secondary electron microscopy (SEM) to highlight the presence of the nanoparticles in the core of fiber samples. Care was taken to check that the observed particles are not artifacts of the carbon coating by using secondary-electron-based images in addition to backscattered-electron-based images. Backscattered-electron-based SEM images are shown on Figure 3 and confirm the presence of particles for fiber samples containing 1 atom % of La (on the left) or 2.1 atom % of Mg (on the right). Magnesium-rich particles in the SEM image on the right appear less clear than the lanthanum-rich particles (on the left) because the chemical contrast between magnesium and silica is lower than that between lanthanum and silica. The origin of the elongated particles in both images is discussed in previous papers [16,17]. Figure 2 shows the increase in the La content along the length of the optical fiber, which is in agreement with the increasing soaking time with the second doping solution. The same gradual whitening is observed in the Mg-doped preform. Mg content ranges between 0.2 and 2.7 atom % for the analyzed fiber samples. La content varies between 0.1 and 1 atom %. To highlight the effect of the nanoparticles, a reference sample was also used. This silica-based reference fiber is slightly doped with GeO_2 and P_2O_5 for the guiding properties of the optical fiber and Er^{3+} ions for its reference spectra in silica. The exact concentrations of Ge and P are not known, but they are in the typical range (≈mol %) for optical fibers used in telecommunications and in agreement with the refractive index difference between the core of the optical fiber and the cladding, which is 0.003 [18,19].

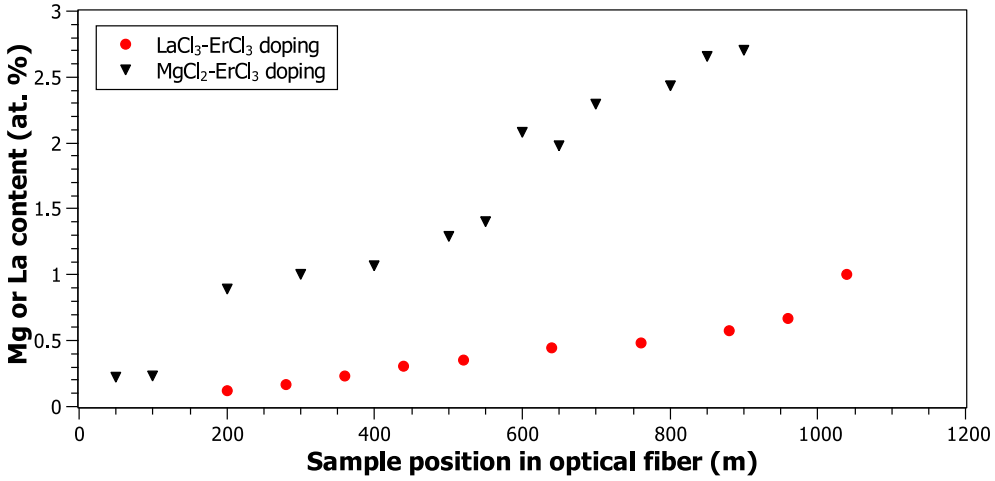

Figure 2. Magnesium and lanthanum contents for analyzed gradual-doping fiber samples.

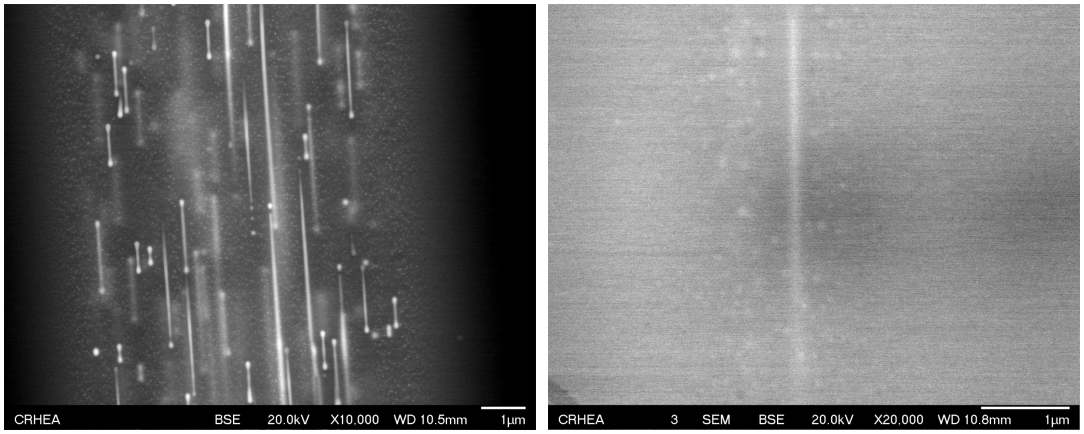

Figure 3. Secondary electron microscopy (SEM) images of the core of two optical fiber samples. The core sections correspond to the longitudinal view (along the drawing axis). The image on the left shows the core of the La-doped sample containing 1 atom % of La. The image on the right shows the highly doped part of the core of the Mg-doped sample containing 2.1 atom % of Mg.

Optical losses were measured by the cutback method with a cutback length of 2 cm, and refractive index liquid was used to remove light from the cladding. Optical loss values at 900 and 1100 nm were chosen for comparisons. These wavelengths were selected as background values because they are far from the $^4I_{11/2}$ and $^4I_{13/2}$ absorption bands of Er^{3+}. Spontaneous emission spectra from the $^4I_{13/2}$ level of Er^{3+} were measured in reference and co-doped samples (Mg and La). A wavelength division multiplexer (WDM) was used to pump fibers at 980 nm and to collect the contra-propagative emission spectra of the $^4I_{13/2}$ level of Er^{3+}, around 1540 nm. Emission spectra measurements were conducted on 0.5 cm long fiber samples at room temperature.

3. Results and Discussions

3.1. Optical Losses

Optical losses at 900 and 1100 nm are displayed in Figure 4 for La- and Mg-doped fiber samples. For both fibers, the same trend is observed at both wavelengths for the evolution of the optical losses with Mg and La content. First, a plateau between 0.1 and 1 dB/m is observed for the optical losses until 0.5 atom % of La and 1.5 atom % of Mg. Then, an increase in optical losses is observed with

increasing Mg and La content. Increases of up to 5300 and 320 $dB \cdot m^{-1}$ are observed for La and Mg doping, respectively. Refractive index mismatch was measured to be between 0.004 for low La content and 0.012 for up to around 1 atom % of La, and it ranges between 0.004 and 0.006 for between 0.2 and 1.3 atom % of Mg. Numerical aperture is between 0.11 and 0.19, which has little influence on the values of optical losses measured by the cutback method [20] (p. 413). All refractive index profiles present the standard MCVD central depletion in germanium, which, therefore, cannot be responsible for such an increase in optical losses. However, it has been reported previously that when Mg or La content increases, the size of nanoparticles increases too in the core of the optical fibers [16]. Then, the increasing value of optical losses is attributed to the increasing size of the nanoparticles as they induce light scattering [10,16]. In the case of lanthanum, particles are clearly observed by SEM from a content of around 3000 atomic ppm of La [10,16]. In the case of magnesium, no clear evidence of the presence of nanoparticles is observed for concentrations lower than 2 atom % of Mg.

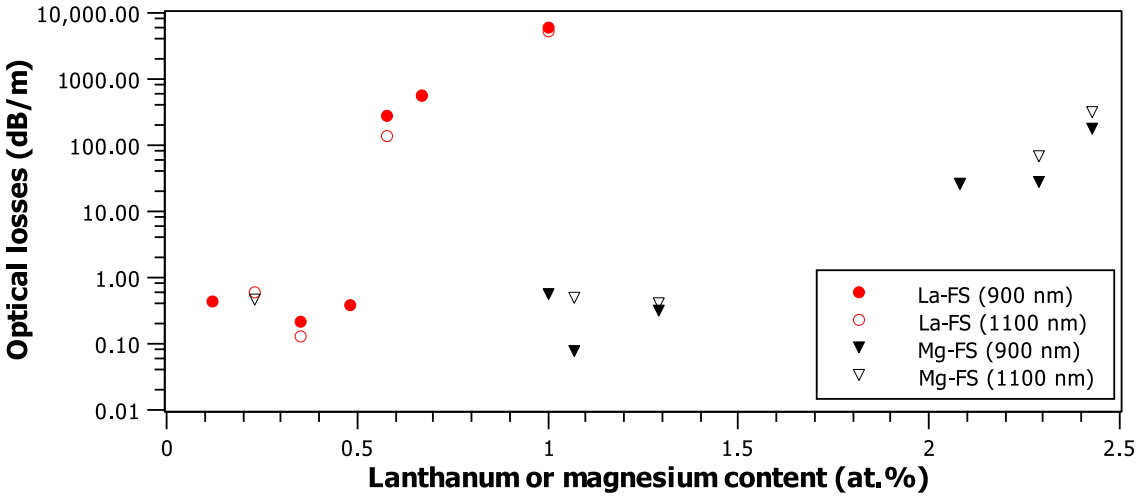

Figure 4. Optical losses of lanthanum- and magnesium-doped fiber samples measured at 900 and 1100 nm.

3.2. Spontaneous Emission Spectra

Figure 5 shows normalized emission spectra of magnesium-doped and reference samples. Area-normalized spectra are normalized over the 1450–1640 nm region. The high limit of 1640 nm was chosen for comparison purposes with samples from the study of D'Acapito et. al. Both area-normalized and maximum-normalized spectra are shown for the Ref-silica sample and samples containing between 0.2 and 2.7 atom % of Mg. Emission spectra shapes are clearly different between magnesium-doped samples and the Ref-silica fiber sample.

In the case of lanthanum-doped samples, emission spectra are reported in Figure 6. The spectra of the silica reference sample is also shown in Figure 6.

It is possible to notice that the variation in La content from undetectable up to 1 atom % induces a variation in the emission profile (cf. Figure 6) that is stronger than the variation in the emission profile with the increase in Mg content from 0.2 up to 2.7 atom % (cf. Figure 5). The higher the content of lanthanum, the wider the maximum-normalized emission spectra. Also, it appears that an increase in lanthanum content increases the height of the high-intensity peak relative to the rest of the spectrum. The second high-intensity peak around 1.55 µm increases from 0.46 to 0.64 a.u. with an increase in lanthanum content.

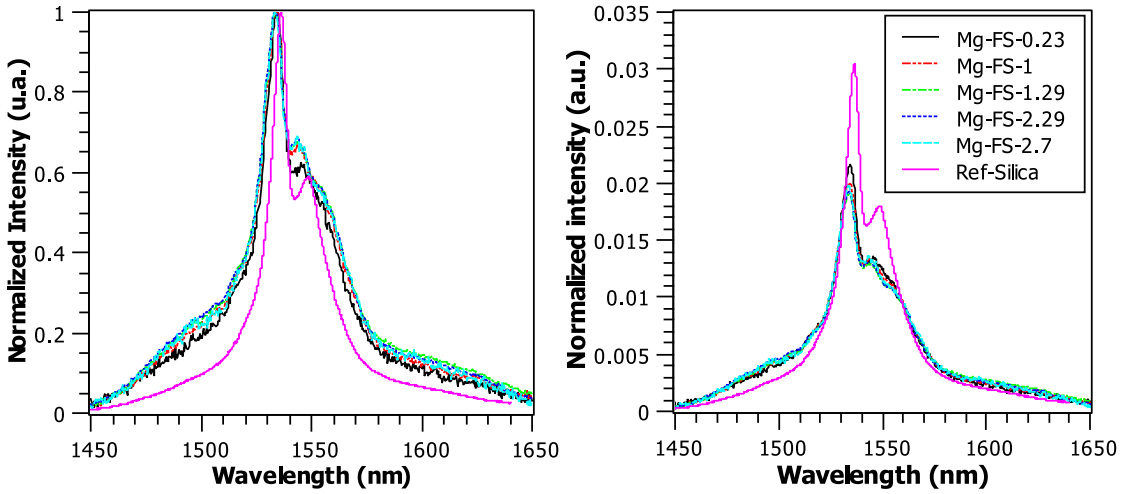

Figure 5. Maximum-normalized (**on the left**) and area-normalized **(on the right**) Er^{3+} emission spectra of magnesium-doped samples. Samples are labeled according to their content in magnesium.

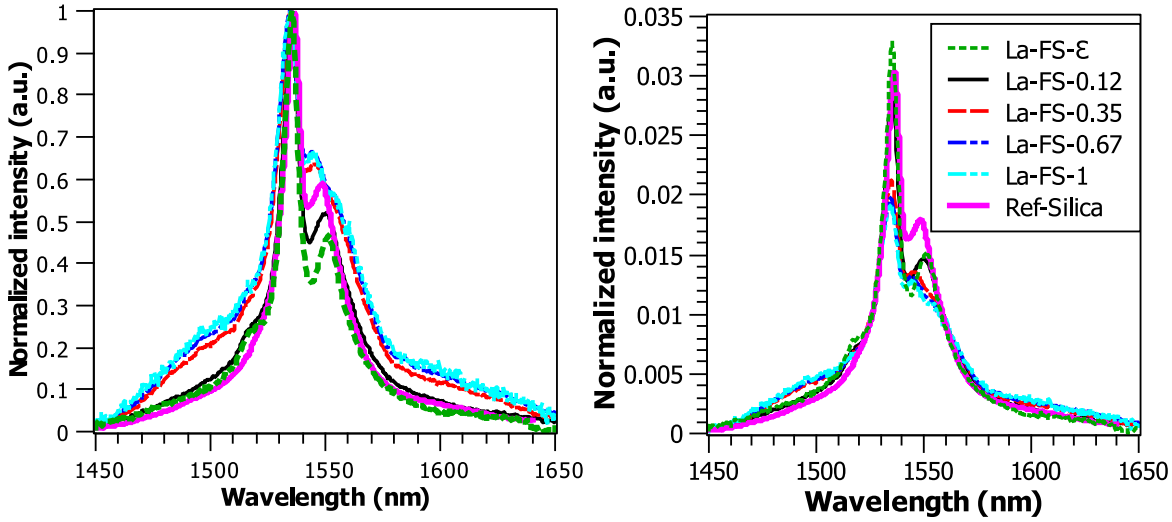

Figure 6. Maximum-normalized (**on the left**) and area-normalized (**on the right**) Er^{3+} emission spectra of lanthanum-doped samples. Samples are labeled according to their content in lanthanum; ϵ is used for the sample where lanthanum content was too low to be measurable.

Figure 7 shows the emission spectra that were normalized by maximum intensities. This figure enables comparison of the emission spectra of the Mg- and La-doped samples. Modification of the spectra is expected to result from an inhomogeneous broadening of the sublevels of the $^4I_{13/2}$ and $^4I_{15/2}$ manifolds of Er^{3+}. This broadening (cf. Figures 5 and 6), compared with the Ref-silica sample, is proposed to result from enrichment in Mg or La of the surroundings of the Er^{3+} ions, as observed in the case of Ca and Mg by D'Acapito et al. [14,21].

For both Mg- and La-doped fiber samples, the peak wavelength at the highest emission intensity was measured. Figure 8 shows the peak wavelength as a function of lanthanum or magnesium content. Increasing magnesium and lanthanum concentration induces an overall blue shift of the peak wavelength, with the peak wavelength of the Ref-silica sample at 1536.4 nm. For lanthanum-doped samples, the increase in lanthanum content induces a peak wavelength shift from 1535.2 nm for 0.1 atom % La down to 1534.8 for 1 atom % La. The maximum and minimum measured peak wavelengths are 1535.6 nm and 1534.6 nm. In the case of magnesium doping, Figure 8 shows a monotonic decrease

in the peak wavelength with Mg content. A shift from 1534.4 nm for 0.2 atom % Mg down to 1533.6 nm for 2.7 atom % Mg is observed.

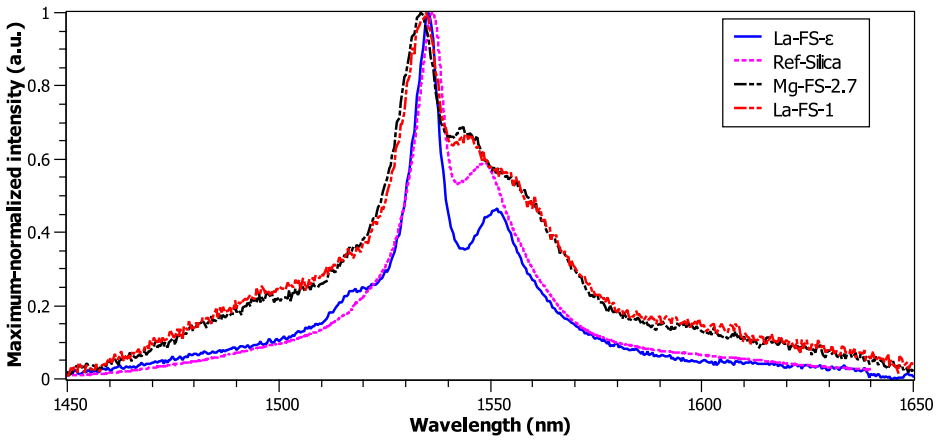

Figure 7. Comparison of the maximum normalization of Er^{3+} emission spectra of the $^4I_{13/2}$ level in fiber samples. Emission spectra of highly doped Mg and La fiber samples are displayed with Ref-silica and low La content samples.

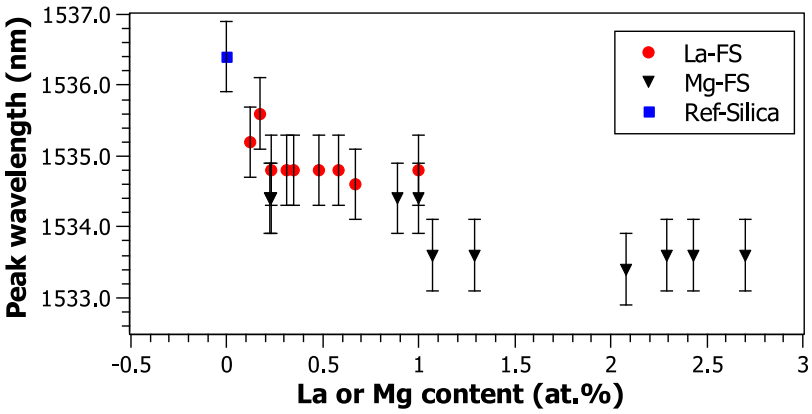

Figure 8. Emission peak wavelengths for fiber samples (FS) as a function of magnesium or lanthanum content.

3.3. Width of Emission Band

One objective of this article is to assess the effect of the doping element (magnesium or lanthanum) and content on the spectroscopic properties, namely, the width of emission band issued from the $^4I_{13/2}$ level of Er^{3+}. However, the $^4I_{13/2} \rightarrow {}^4I_{15/2}$ emission of Er^{3+} in the telecom band is known to have a non-neglectable variation in the oscillator strengths of its Stark levels [22]. Considering the important profile variations in the emission spectra, care was taken with the choice in the characterization method of the emission's width.

Characterization of the width of emission band has been already discussed for the case of magnesium and phosphorous doping of silica by d'Acapito et al. [14]. The width of the emission band was defined as the full-width at half-maximum (FWHM). In our study, the emission spectra of the various fiber samples enabled the observation of the complexity of the quantification of the emission band's broadening. Indeed, increasing the doping content of the fiber samples not only enlarges the emission band but also induces strong profile modifications. For example, the relative intensity between the two high-intensity peaks varies between 0.46 and 0.65 for La-FS-ϵ (non-measurable

content of lanthanum) and La-FS-1, and reaches up to 0.69 for Mg-FS-2.7. The relative height of the second peak is 0.59 for the Ref-silica sample. Considering the evolution of the emission profile with La doping, FWHM suffers from an artifact caused by the ratio of the two high-intensity peaks reaching values below 0.5.

$$\Delta\lambda_{eff} = \frac{\int I(\lambda)d\lambda}{I_{max}} \quad (1)$$

To account for these strong profile modifications, the effective linewidth $\Delta\lambda_{eff}$ is proposed to be used to compare the emission bandwidths. The effective linewidth corresponds to the area of the spectrum divided by its maximum intensity I_{max} (cf. Equation (1)), as defined by Weber and used by Jiang et al. [23,24]. The fact that the effective linewidth is based on the area of the spectrum and the maximum intensity provides a means of comparison of the width that is more robust with the strong variations in spontaneous emission profiles of around half of the maximum intensity. Considering the use of both FWHM and effective linewidth in previous studies, both characterizations are discussed.

In the case of FWHM, Figure 9 shows that the width of the emission band evolves with the same trend as for the $\Delta\lambda$-defined width, between 21.4 nm for the Ref-silica sample, around 31–32 nm for lanthanum doping's FWHM plateau value, and around 34–35 nm for the magnesium doping's FWHM plateau value. However, because of the relative intensity of the second peak, as discussed before, La-FS-0.12 has an FWHM of 11 nm, contrasting with the rest of the results.

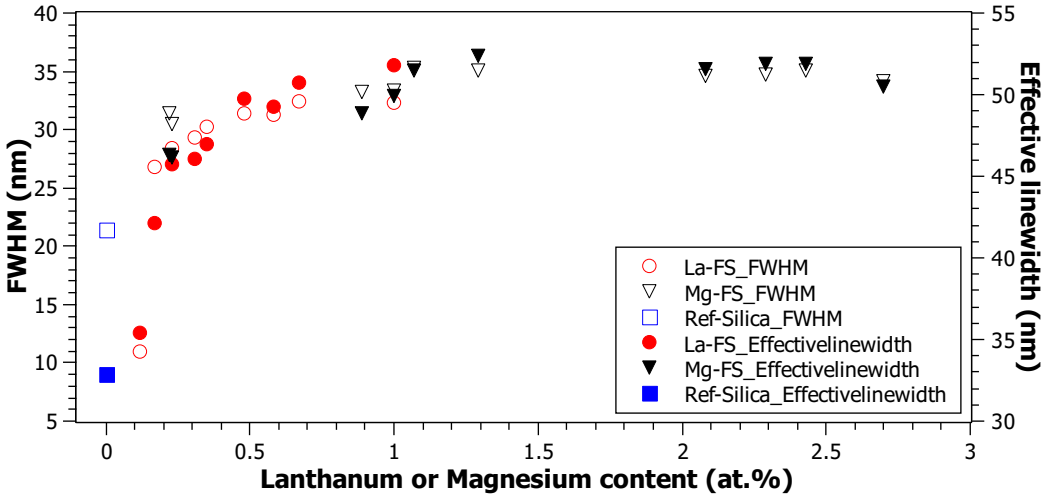

Figure 9. Evolution of Er^{3+} emission bandwidth with lanthanum (black) and magnesium (red) content. Ref-silica values are shown in blue. Circle symbols are used for the effective linewidth (on the right scale) and crosses are used for FWHM (on the left scale).

For $\Delta\lambda_{eff}$, Figure 9 shows, using plain symbols, the evolution of the $\Delta\lambda_{eff}$ with respect to the Mg and La content. There is an overall monotonic increase in the $\Delta\lambda_{eff}$ with increasing doping content up to a plateau. For Mg-doped fibers, the width $\Delta\lambda_{eff}$, defined in the previous section, is relatively invariant with Mg content. The width increases from 46.3 up to a plateau of 51–52 nm with a variation in magnesium content from 0.22 to 2.7 atom %. In the case of lanthanum, the emission band's width increases from 35.5 to 52 nm for between 0.1 and 1 atom % of La. For the analyzed samples, the width $\Delta\lambda_{eff}$ increases up to ≈52 nm with increasing La or Mg co-doping content, compared with the 32.8 nm measured in the silica reference sample.

Figure 10 shows the evolution of the width $\Delta\lambda_{eff}$ as a function of the optical losses for the lanthanum- and magnesium-doped fibers. In the case of lanthanum, a plateau value of the emission effective linewidth $\Delta\lambda_{eff}$ is reached at above 1 dB·m^{-1} of optical losses for concentrations higher than

0.35 atom %. We recall here that a value of 0.1 dB·m^{-1} can be compatible with fiber laser and amplifier applications [10]. In the case of magnesium doping, the variation is lower, which is in agreement with the emission spectra. The emission remains constant at around a plateau value of 35.4 nm from optical losses inferior to 0.1 dB·m^{-1} or for Mg concentrations higher than 1.1 atom %. In both cases, the plateau values are quite similar. For optical losses of around 0.1 dB·m^{-1}, Mg allows for a greater broadening of the emission spectra, with 35 and 51 nm for FWHM and effective linewidth, respectively, compared with 30.2 and 47 nm for FWHM and effective linewidth, respectively, for co-doping with lanthanum. Thus, magnesium is more interesting for its ability to broaden the 1.5 µm Er^{3+} emission band with lower optical losses than lanthanum.

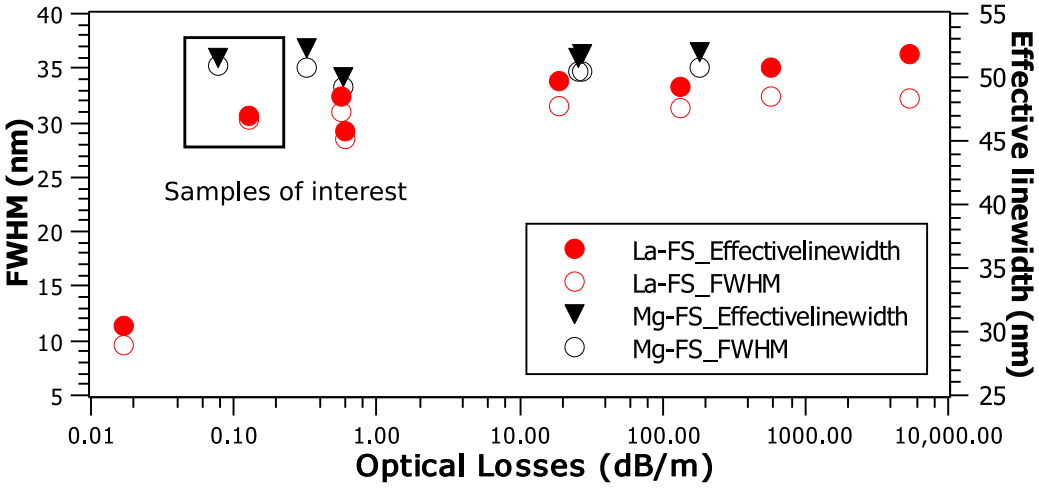

Figure 10. Evolution of Er^{3+} emission width with optical losses measured at 900 nm for lanthanum and magnesium co-doping.

The results presented in this paper clearly show the broadening effect of the formation of Mg- and La-rich nanoparticles on the $^4I_{13/2}$ emission of Er^{3+}-doped fibers. Even more, results show that it is possible to obtain fiber samples with enhanced properties with acceptable optical losses (below 0.1 dB·m^{-1}). Using phosphorous would allow one to further increase the broadening of the emission [14]. However, interactions between phosphorous with other doping elements (such as magnesium) are complex, and its effects on optical losses are not known [14]. Therefore, the present work also provides important data for further investigations on the effect of phosphorous.

4. Conclusions

In conclusion, we prepared nanoparticle-rich erbium-doped optical fiber samples that were co-doped with magnesium or lanthanum. The use of gradual-time solution doping allowed for the fabrication of tens of samples of different concentrations with only two MCVD optical fiber elaborations. The ability of the process to produce nanoparticle-rich fiber samples was evidenced. Optical losses were measured, and the widths of the emission band of the $^4I_{13/2}$ level of Er^{3+} were characterized for the fiber samples. The complex characterization of the emission bandwidth was explored, and both FWHM and effective linewidth were used in this study. Results show that both lanthanum and magnesium doping allow for an increase in the width of emission. The analysis of results also confirms that magnesium and lanthanum doping induces an increase in the optical losses with the broadening of the emission. For acceptable optical losses, magnesium doping of 1.1 atom % increased the FWHM and effective linewidth up to 35 nm and 51 nm, respectively, and 30 nm and 47 nm, respectively, in the case of 0.35 atom % of lanthanum. Therefore, compared with the Ref-silica sample, fabrication of nanoparticle-rich optical fibers through lanthanum or magnesium doping can induce an FWHM

broadening of 64% and 54%, respectively, or an effective linewidth broadening of 59% (for both doping elements) while maintaining transparency.

Author Contributions: Conceptualization, M.V., J.-F.L. and W.B.; methodology, M.V., J.-F.L., M.U., S.T. and W.B.; validation, M.V., J.-F.L. and W.B.; formal analysis, M.V., J.-F.L. and W.B.; investigation, M.V., J.-F.L. and W.B.; resources, M.U. and S.T.; data curation, W.B.; writing—original draft preparation, M.V.; writing—review and editing, M.V. and W.B.; visualization, M.V., J.-F.L. and W.B.; supervision, W.B.; project administration, W.B.; funding acquisition, W.B.", please turn to the CRediT taxonomy for the term explanation. Authorship must be limited to those who have contributed substantially to the work reported.

Funding: Université Nice Sophia Antipolis, Centre National de la Recherche Scientifique, Agence Nationale de la Recherche (ANR-14-CE07-0016-01, Nice-DREAM).

Conflicts of Interest: The authors declare no conflict of interest.

References

1. Richardson, D.; Nilsson, J.; Clarkson, W. High power fiber lasers: current status and future perspectives. *JOSA B* **2010**, *27*, B63–B92. [CrossRef]
2. Ballato, J.; Ebendorff-Heidepriem, H.; Zhao, J.; Petit, L.; Troles, J. Glass and process development for the next generation of optical fibers: A review. *Fibers* **2017**, *5*, 11. [CrossRef]
3. Digonnet, M.J. (Ed.) *Rare-Earth-Doped Fiber Lasers and Amplifiers*; CRC Press: Boca Raton, FL, USA, 2001.
4. Sudarsan, V.; Van Veggel, F.C.; Herring, R.A.; Raudsepp, M. Surface Eu^{3+} ions are different than "bulk" Eu^{3+} ions in crystalline doped LaF^3 nanoparticles. *J. Mater. Chemi.* **2005**, *15*, 1332–1342. [CrossRef]
5. Gonçalves, M.C.; Santos, L.F.; Almeida, R.M. Rare-earth-doped transparent glass ceramics. *C. R. Chim.* **2002**, *5*, 845–854.
6. Faure, B.; Blanc, W.; Dussardier, B.; Monnom, G. Improvement of the Tm^{3+}: $^3H_4$ level lifetime in silica optical fibers by lowering the local phonon energy. *J. Non-Cryst. Solids* **2007**, *353*, 2767–2773. [CrossRef]
7. Lupi, J.F.; Vermillac, M.; Blanc, W.; Mady, F.; Benabdesselam, M.; Dussardier, B.; Neuville, D.R. Impact of cerium and lanthanum on the photo-darkening and photo-bleaching mechanisms in thulium-doped fibre. *Opt. Mater.* **2017**, *72*, 106–114. [CrossRef]
8. Lupi, J.F.; Vermillac, M.; Blanc, W.; Mady, F.; Benabdesselam, M.; Dussardier, B.; Neuville, D.R. Steady photodarkening of thulium alumino-silicate fibers pumped at 1.07 μm: Quantitative effect of lanthanum, cerium, and thulium. *Opt. Lett.* **2016**, *41*, 2771–2774. [CrossRef]
9. Mebrouk, Y.; Mady, F.; Benabdesselam, M.; Duchez, J.B.; Blanc, W. Experimental evidence of Er^{3+} ion reduction in the radiation-induced degradation of erbium-doped silica fibers. *Opt. Lett.* **2014**, *39*, 6154–6157. [CrossRef]
10. Vermillac, M.; Fneich, H.; Lupi, J.F.; Tissot, J.B.; Kucera, C.; Vennéguès, P.; Mehdi, A.; Neuville, D.R.; Ballato, J.; Blanc, W. Use of thulium-doped LaF3 nanoparticles to lower the phonon energy of the thulium's environment in silica-based optical fibres. *Opt. Mater.* **2017**, *68*, 24–28. [CrossRef]
11. Kucera, C.; Kokuoz, B.; Edmondson, D.; Griese, D.; Miller, M.; James, A.; Baker, W.; Ballato, J. Designer emission spectra through tailored energy transfer in nanoparticle-doped silica preforms. *Opt. Lett.* **2009**, *34*, 2339–2341. [CrossRef]
12. Kasik, I.; Peterka, P.; Mrazek, J.; Honzatko, P. Silica optical fibers doped with nanoparticles for fiber lasers and broadband sources. *Curr. Nanosci.* **2016**, *12*, 277–290. [CrossRef]
13. Blanc, W.; Guillermier, C.; Dussardier, B. Composition of nanoparticles in optical fibers by Secondary Ion Mass Spectrometry. *Opt. Mater. Express* **2012**, *2*, 1504–1510. [CrossRef]
14. D'Acapito, F.; Blanc, W.; Dussardier, B. Different Er3+ environments in Mg-based nanoparticle-doped optical fibre preforms. *J. Non-Cryst. Solids* **2014**, *401*, 50–53. [CrossRef]
15. Lupi, J.F.; Vermillac, M.; Trzesien, S.; Ude, M.; Blanc, W.; Dussardier, B. Gradual-time solution doping for the fabrication of longitudinally varying optical fibres. *J. Lightw. Technol.* **2018**, *36*, 1786–1791. [CrossRef]
16. Vermillac, M.; Fneich, H.; Turlier, J.; Cabié, M.; Kucera, C.; Borschneck, D.; Peters, F.; Vennéguès, P.; Neisius, T.; Chaussedent, S.; et al. On the morphologies of oxides particles in optical fibers: Effect of the drawing tension and composition. *Opt. Mater.* **2018**, in press. [CrossRef]

17. Vermillac, M.; Lupi, J.F.; Peters, F.; Cabie, M.; Vennegues, P.; Kucera, C.; Neisius, T.; Ballato, J.; Blanc, W. Fiber-draw-induced elongation and break-up of particles inside the core of a silica-based optical fiber. *J. Am. Ceram. Soc.* **2017**, *100*, 1814–1819. [CrossRef]
18. Schultz, P. Ultraviolet absorption of titanium and germanium in fused silica. In Proceedings of the Eleventh International Congress on Glass, Prague, Czech Republic, 4–8 July 1977.
19. Schultz, P.C. Fused P_2O_5 Type Glasses. U.S. Patent 4,042,404, 16 August 1977.
20. Ghatak, A.; Thyagarajan, K. *An Introduction to Fiber Optics*; Cambridge University Press: Cambridge, UK, 1998.
21. D'Acapito, F.; Maurizio, C.; Paul, M.C.; Lee, T.S.; Blanc, W.; Dussardier, B. Role of CaO addition in the local order around Erbium in SiO_2–GeO_2–P_2O_5 fiber preforms. *Mater. Sci. Eng. B* **2008**, *146*, 167–170. [CrossRef]
22. Wade, S.A.; Collins, S.F.; Baxter, G.W. Fluorescence intensity ratio technique for optical fiber point temperature sensing. *J. Appl. Phys.* **2003**, *94*, 4743–4756. [CrossRef]
23. Weber, M. Optical materials, Part 1-Nonlinear optical properties/radiation damage. In *CRC Handbook of Laser Science and Technology*; CRC Press: Boca Raton, FL, USA, 1986; Volume 3.
24. Jiang, S.; Luo, T.; Hwang, B.C.; Smekatala, F.; Seneschal, K.; Lucas, J.; Peyghambarian, N. Er^{3+}-doped phosphate glasses for fiber amplifiers with high gain per unit length. *J. Non-Cryst. Solids* **2000**, *263*, 364–368. [CrossRef]